Shape-from-Shadow Building Reconstruction from Multiple View SAR Images [1)]

Regine Bolter and Franz Leberl
Computer Graphics and Vision
Graz University of Technology
A- 8010 Graz, Inffeldgasse 16/II, Austria
Tel.: +43 316 873 5024, Fax: +43 316 873 5050
E-mail: bolter@icg.tu-graz.ac.at

Abstract:
Detection and geometric reconstruction of man-made objects from high resolution, multiple view interferometric SAR data gets feasible. IFSAR data is corrupted by blur, speckle noise, and other view dependent effects as e.g., layover and shadows. Especially in case of buildings, these phenomenological features may also provide valuable information about the underlying structure. In this paper we focus on the reconstruction of building walls from multiple view slant range shadows. The exact segmentation of the shadow boundaries is the crucial task of this process. This is accomplished using a rotating mask for edge detection. The mask exploits textural differences between adjacent regions. From the segmented shadow boundaries, the building outlines are reconstructed. The results correspond well to the ground truth data, especially the building's areas are delimited better than from interferometric data.

1 Introduction

The motivation for our work is the rapidly growing availability of interferometric radar data sources at very high geometric resolutions. Data types are being produced in a single view such as an interferogram representing noisy approximations of 3D shape, a magnitude image representing a noisy analogy to an optical image, and a coherence image describing the surface characteristics of objects. Multiple views add the opportunity to use additional shape-from-X methods to enhance robustness, accuracy and completeness, but require an ability to overcome geometric disparities and radiometric dissimilarities.

Previous demonstrations of such measurements from SAR data were based on manual work,

[1)]The authors wish to thank SANDIA for providing the SAR images and Bob Wilson from Vexcel Corporation for providing the ground truth data.

some limited automated methods can be found. In [9] fusion of IFSAR and multispectral optical image data results in boundary boxes of buildings. [7] describes an automated region growing approach to localize buildings starting from the shadows they cast. The reconstruction of building shapes of urban tower blocks from IFSAR data by applying a range segmentation algorithm is presented in [5]. Techniques for removing artifacts that are peculiar to IFSAR data are discussed in [4].

In contrast to these previous demonstrations, which were performed on a single data source we want to employ the best source for each single measurement and combine the results in an intelligent way. To study the various effects present in SAR data we set up a work environment with a simulator to produce slant range and interferometric SAR data. The slant range magnitude simulator and the reconstruction of a single house from shadows casted in multiple view simulated and real data is presented in [1]. Simulation and multiple view combination of interferometric height data is described in [3]. [2] describes the detection of buildings from multiple view combined interferometric height and coherence data, simple building models are fit to the height measurements within the detected building areas and compared to ground truth data available from optical imagery. Although the height measurements from this interferometric data correspond well to the ground truth data, the areas of the detected buildings from interferometric data differ significantly from the actual values. Small buildings tend to be underestimated, larger buildings are overestimated due to the front porch effect [4].

To improve the measurements of the buildings dimensions this paper will focus on a shape-from-shadow approach for building reconstruction from multiple view slant range magnitude SAR images to enhance the results obtained from interferometry. The correct segmentation of the shadow-boundaries is the crucial task in this process.

2 Test Data

For the detection and reconstruction of buildings test data from the McKenna MOUT site, Ft.Benning, GA is used. The buildings on this site are clustered in a compact group resembling a northern European village, surrounded by undeveloped land. An optical image of the testsite can be seen from Figure 1. From an airborne Sandia Spotlight IFSAR sensor the testsite was imaged from four cardinal azimuth directions. The original slant range magnitude images have a resolution of 0.23 m. The interferometric processing was done by Sandia, each pass was processed into four channels: magnitude, correlation, height and bin number, and converted to UTM coordinates with a resolution of 0.4 m.

An ARC/INFO data set of the Fort Benning MOUT site is used as the ground truth to evaluate the building extraction results. This data set contains the UTM coordinates of building corners, building areas, perimeters as well as building heights, etc.

Figure 1: Optical image of the Ft. Benning MOUT testsite

3 Methods

SAR sensors are range measuring devices. Microwave pulses are transmitted to the side, perpendicular to the flight path and the reflected energy from the ground is recorded in distinct time intervals. Basic SAR imaging properties can be found in e.g., [8]. Shadow is a special phenomenon which occurs in SAR images if a terrain feature is blocking the line of sight between the sensor and the following terrain.

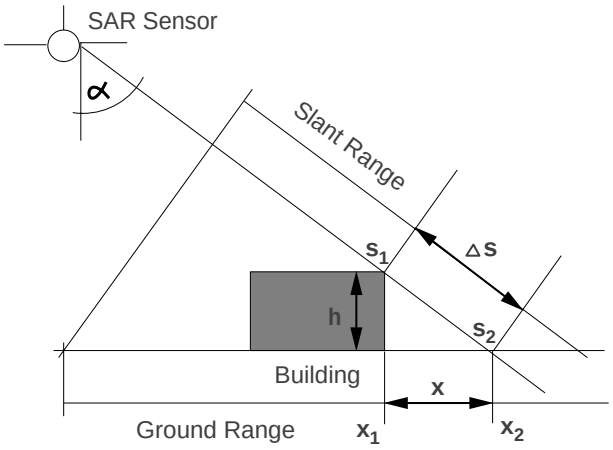

Figure 2: Slant range shadow reconstruction geometry

Figure 2 shows this situation for a simple rectangular object. No reflections will be received at the antenna during the time that signals should be returning from the area between points s_1 and s_2 but no objects are hit between these two points, the radiation is blocked by the vertical structure. On the image, area Δs will be black, called a shadow of the vertical structure. Although shadow areas contain no information, geometrical properties of the shadow areas can be exploited to reconstruct the geometry of the underlying object. In case of buildings with upright walls, from the position and length of the shadows in a single slant range image,

one can calculate the position and height of all walls facing away from the sensor. According to Figure 2 first the shadow endpoint s_2 must be translated in ground range projection x_2, therefrom position x_1 and height of the wall h (in pixel dimensions) can be computed:

$$x_2 = \frac{s_2}{\sin\alpha} \tag{1}$$

$$x_1 = x_2 - \Delta s \sin\alpha \tag{2}$$

$$h = \Delta s \cos\alpha \tag{3}$$

The accurate segmentation of the shadow boundaries is the crucial point to an exact reconstruction. In our test dataset the radiometric resolution of the slant range images is quite poor, only seven different greylevels occur. Due to the SAR imaging principle usually no signal is received from shadow areas, however some noise is present in these quite dark homogeneous regions. A single threshold segmentation is not sufficient, texture measures and speckle statistics have to be taken into account. Speckle is often modeled as a multiplicative random noise which follows a Rayleigh probability distribution [6].

Textural differences between adjacent regions are exploited using 7 by 7 pixel masks to enhance shadow edges. The masks were generated by rotating a simple transition between two regions around 360 degrees, we used 16 rotation steps. The first three rotating masks are as follows:

$$\begin{bmatrix} x & 1 & 1 & 1 & 0 & 0 & 0 \\ x & 1 & 1 & 1 & 0 & 0 & 0 \\ x & 1 & 1 & 1 & 0 & 0 & 0 \\ x & 1 & 1 & 1 & 0 & 0 & 0 \\ x & 1 & 1 & 1 & 0 & 0 & 0 \\ x & 1 & 1 & 1 & 0 & 0 & 0 \\ x & 1 & 1 & 1 & 0 & 0 & 0 \end{bmatrix} \begin{bmatrix} x & 1 & 1 & 0 & 0 & 0 & 0 \\ x & 1 & 1 & 0 & 0 & 0 & 0 \\ x & 1 & 1 & 1 & 0 & 0 & 0 \\ x & 1 & 1 & 1 & 0 & 0 & 0 \\ x & 1 & 1 & 1 & 0 & 0 & 0 \\ x & 1 & 1 & 1 & 1 & 0 & 0 \\ x & 1 & 1 & 1 & 1 & 0 & 0 \end{bmatrix} \begin{bmatrix} 1 & 0 & 0 & 0 & 0 & 0 & 0 \\ 1 & 1 & 0 & 0 & 0 & 0 & 0 \\ 1 & 1 & 1 & 0 & 0 & 0 & 0 \\ 1 & 1 & 1 & 1 & 0 & 0 & 0 \\ 1 & 1 & 1 & 1 & 1 & 0 & 0 \\ 1 & 1 & 1 & 1 & 1 & 1 & 0 \\ x & x & x & x & x & x & x \end{bmatrix}$$

The 'x' in these rotating masks denote don't cares, they were introduced to ensure that the sum of zeros and ones equals in each single mask. We are interested in edge pixels that lie between dark, homogeneous shadow regions and brighter regions of stronger intensity variations. For each pixel in the image mean and variance of the greylevels g for all 16 rotation masks around this central pixel were calculated for both regions separately and the difference in these measurements is exploited:

$$edgestrength = \frac{\overline{g_1} - \overline{g_0}}{255} + \frac{var(g_1) - var(g_0)}{30000} \tag{4}$$

Thresholds are introduced to the mean and variance measurements before this difference is computed. If more than three pixels are nonzero in the area considered as shadow, the mean

value in this area $\overline{g_0}$ is set to 100. For the mean value in the area considered as non shadow $\overline{g_1}$ the minimum of the actual value and 21 is chosen. The same is done for the variance in the non shadow area $var(g_1)$, the minimum of the actual value and 40 is chosen. These thresholds ensure that the difference is above zero only for regions where both criteria are fulfilled, namely the shadow region is dark and homogeneous and the remaining region is non-dark and more inhomogeneous. Each pixel in the image is set to the maximum difference value between the values obtained from the 16 rotation masks. Edge pixels are then selected with a threshold from this maximum edge strength values.

4 Results

This segmentation procedure was applied to all four independent view slant range SAR images. Figure 3 shows on the upper left a subscene of one original slant range SAR image, the sensor imaged the scene left looking from the lower right corner to the upper right corner as seen

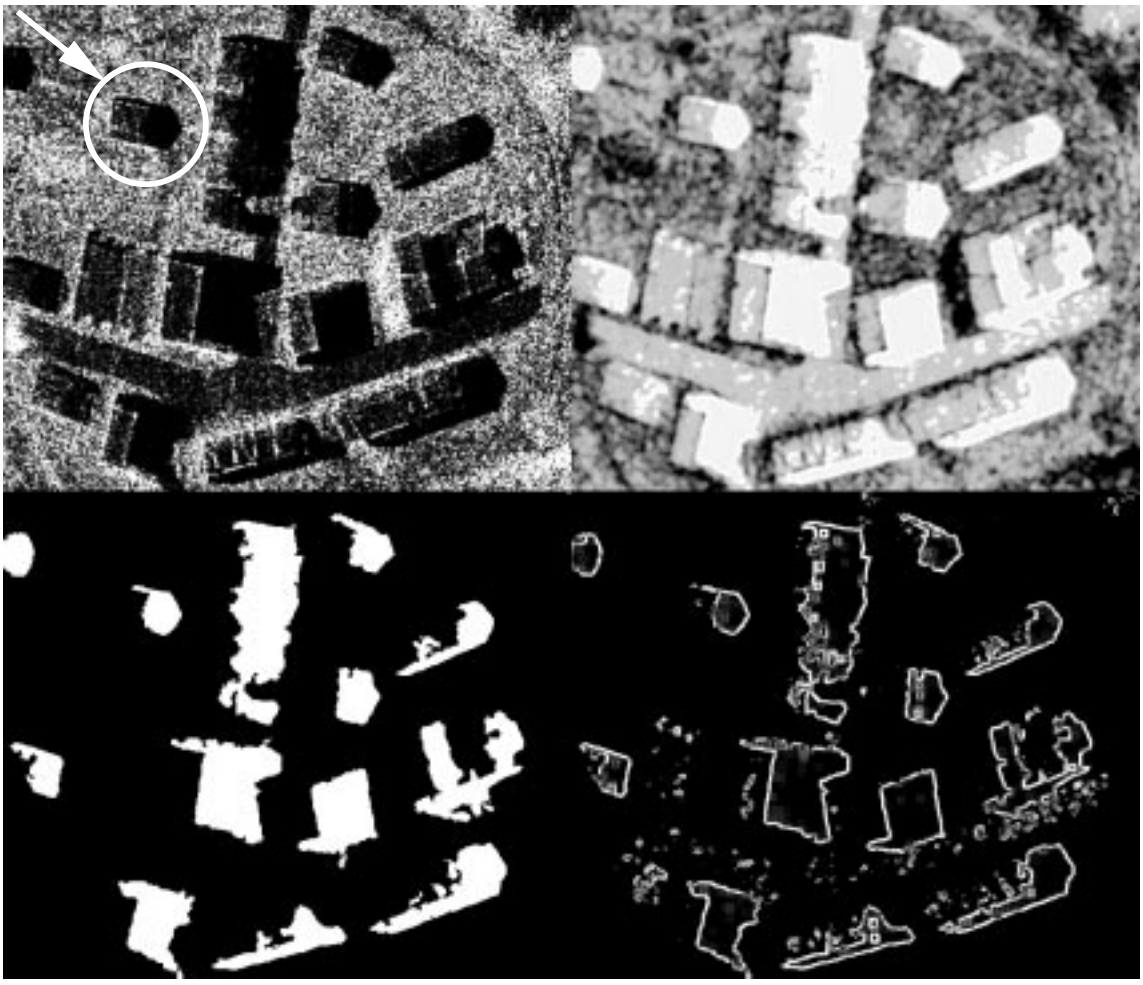

Figure 3: Clockwise from upper left: Subscene of original slant range SAR image, edge filter response, edge filter response above zero and resulting regions. The area covers 150 x 100 m^2.

from the optical image of the scene in Figure 1. The resulting filter response for the difference criteria is shown on the upper right image in Figure 3. On the lower right of Figure 3 only filter response values above zero are shown. This results in closed borders for all shadow regions casted from the buildings in the scene. Therefore a single threshold above zero is sufficient to segment the shadow areas. In the lower left image of Figure 3 the resulting segmented regions are shown. These regions were derived by first deleting small regions with less than 100 pixels after thresholding the edge pixels above zero and than filling the resulting closed borders.

From these segmented shadow boundaries the building walls can be reconstructed, as described in the methods section. The assumption of upright walls and flat terrain surrounding the walls is valid for our test data. The reconstruction of the walls is demonstrated for the circled building in the upper left of Figure 3. For each image line start- and endpoints of all shadow regions within this line are marked, and position and height of the walls represented by these shadows are calculated in ground range projection according to the Equations (1-3). Figure 4 shows in the upper row the segmented shadow of this building from four independent views, in the lower row the reconstructed walls from these shadows can be seen, brighter pixels correspond with higher elevations

Figure 4: Segmented shadows of a single building in four independent views and reconstructed walls facing away from the sensor. The building area covers 13 x 8 m^2, its maximum height is 6.6 m

The four independent views can be combined, after the resulting wall images are resampled in line direction to get square pixels and after rotating the single views according to the actual look direction of the sensor. From the left of Figure 5 the resulting reconstructed building walls for the circled image in Figure 3 can be seen. In the middle of Figure 5 the corresponding outlines of the building from the ground truth data are overlaid to the reconstructed walls. On the left of Figure 5 a shaded view of the resulting building walls can be seen.

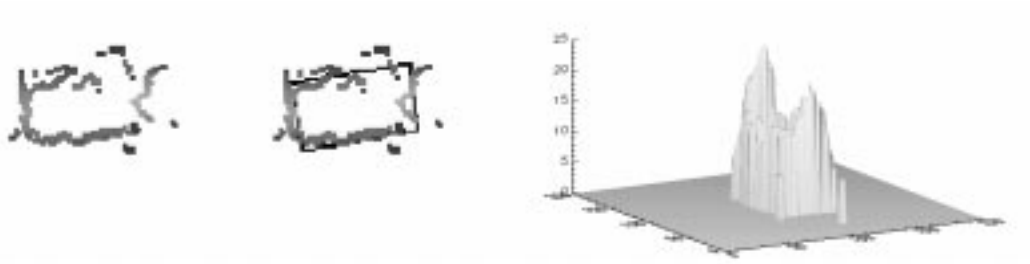

Figure 5: Combination of four independent views for the circled building in Figure 3, overlaid outlines from ground truth data and a shaded view of the reconstructed walls.

Figure 6 shows the resulting reconstruction of the building walls for the whole building ensemble of the MOUT testsite with overlaid building outlines from ground truth data. The building areas resulting from the reconstructed outlines were measured manually. The RMS error of the building areas compared to ground truth is $\pm 27.80 m^2$. This is significantly better compared to the measurements from interferometric data [2], where the remaining RMS area error is $\pm 109.6 m^2$. The resulting RMS error in the maximum height is $\pm 1.86 m$, which is slightly worse compared to the interferometric measurements [2], the resulting maximum height RMS error for the interferometric measurements is $\pm 1.56 m$.

Figure 6: Reconstructed building walls of the whole building ensemble on the MOUT testsite with overlaid building outlines from ground truth data.

5 Discussion and Outlook

The reconstruction of buildings from multiple view high resolution slant range SAR shadows is possible. Shadow manifests itself as quite dark and homogeneous region, segmentation was accomplished using texture measures and a rotating mask filter. However, the resulting contours of the shadow regions remain noisy, some artifacts which do not belong to the shadow area remain in the segmented set. The reconstruction of the building walls depend on the quality of the segmentation. Comparing the resulting building's outlines with ground truth data, as can be seen from Figure 6, shows reasonable correspondence. Problems arise in case of occlusions, when adjacent buildings interfere with the shadow region of the actual building, in this case the resulting walls from the independent views do not form a regular rectangle. Another problem in the reconstruction results from the fact that trees cast shadows in the slant range SAR images, too. A decision process between natural and man-made objects is necessary. However, these measurements from slant range shadows are just one step in the building detection and reconstruction from multiple view high resolution IFSAR images. The decision between trees and buildings can easily be drawn from interferometric height and coherence measurements, as was demonstrated in [2]. The building outlines are better defined from slant range shadows than from interferometric height measurements. The combination of these slant range shadow height measurements with interferometric height measurements remains a topic for further work. It might also help to identify occluded shadows in the slant range image and correct the hight measurements accordingly.

References

[1] R. Bolter. Reconstruction of Man-Made Objects from High Resolution SAR Images. In *Proceedings of IEEE Aerospace Conference*, CD-ROM, Paper No.: 6.0305, 2000.

[2] R. Bolter and F. Leberl. Detection and Reconstruction of Human Scale Features from High Resolution Interferometric SAR data. In *Accepted for Publication in Proceedings of ICPR 2000.*

[3] R. Bolter and F. Leberl. Phenomenology-Based and Interferometry-Guided Building Reconstruction from Multiple SAR Images. In *Proceedings of EUSAR*, 2000.

[4] G. Burkhart, Z. Bergen, and R. Carande. Elevation Correction and Building Extraction from Interferometric SAR Imagery. In *Proceedings of IGARSS'96*, pages 659–661, 1996.

[5] P. Gamba, B. Houshmand, and M. Saccani. Detection and Extraction of Buildings from Interferometric SAR Data. *IEEE T-GRS*, 38(1):611–618, January 2000.

[6] J. Goodman. *J.C. Dainty: Laser Speckle and Related Phenomena*, chapter Statistical Properties of Laser Speckle Patterns. Springer Verlag, Berlin, 1975.

[7] K. Hoepfner, A. Hanson, and E. Riseman. Recovery of Building Structure from SAR and IFSAR Images. In *ARPA Image Understanding Workshop*, pages 559–563, 1998.

[8] F. W. Leberl. *Radargrammetric Image Processing.* Artech House, 1990.

[9] R. Xiao, C. Lesher, and B. Wilson. Building Detection and Localization Using a Fusion of Interferometric Synthetic Aperture Radar and Multispectral image. In *ARPA Image Understanding Workshop*, pages 583–588, 1998.